Computed tomographic myelography for assessment of the cervical spinal cord in ataxic warmblood horses: 26 cases (2015–2017)

Tibor Rovel DVM
Marieke Zimmerman DVM
Luc Duchateau DVM, PhD
Edouard Adriaensen DVM
Tom Mariën DVM
Jimmy H. Saunders DVM, PhD
Katrien Vanderperren DVM, PhD

From the Department of Veterinary Medical Imaging (Rovel, Saunders, Vanderperren), and Biometrics Research Group (Duchateau), Faculty of Veterinary Medicine, Ghent University, 9820 Merelbeke, Belgium; and Equitom Equine Hospital, 3560 Meldert, Belgium (Zimmerman, Adriaensen, Mariën).

Address correspondence to Dr. Rovel (rovel.tibor@gmail.com).

OBJECTIVE
To quantify the degree of dural compression and assess the association between site and direction of compression and articular process (AP) size and degree of dural compression with CT myelography.

ANIMALS
26 client-oriented horses with ataxia.

PROCEDURES
Spinal cord-to-dura and AP-to-cross-sectional area of the C6 body ratios (APBRs) were calculated for each noncompressive site and site that had > 50% compression of the subarachnoid space. Site of maximum compression had the largest spinal cord-to-dura ratio. Fisher exact test and linear regression analyses were used to assess the association between site and direction of compression and mean or maximum APBR and spinal cord-to-dura ratio, respectively.

RESULTS
Mean ± SD spinal cord-to-dura ratio was 0.31 ± 0.044 (range, 0.20 to 0.41) for noncompressive sites and 0.44 ± 0.078 (0.29 to 0.60) for sites of maximum compression. Sites of maximum compression were intervertebral and extradural, most frequently at C6 through 7 (n = 10), followed by C3 through 4 (6). Thirteen horses had dorsolateral and lateral compression at the AP joints, secondary to AP (n = 7) or soft tissue proliferation (6). Site significantly affected direction of compression, and directions of compression from occiput through C4 were primarily ventral and lateral, whereas from C6 through T1 were primarily dorsal and dorsolateral. No linear relationship was identified between mean or maximum APBR and spinal cord-to-dura ratio.

CONCLUSIONS AND CLINICAL RELEVANCE
CT myelography may be useful for examination of horses with suspected cervical compressive myelopathy. Degree of compression can be assessed quantitatively, and site of compression significantly affected direction of compression.

Cervical compressive myelopathy (CCM) and subsequent development of ataxia have been extensively reported in horses,[1–6] and CCM is the most commonly reported cause of ataxia in horses in Europe and Australia.[4] Two types of CCM have been described[7,8]: dynamic compression of the cranial portion of the cervical spine (C2 through C4) that generally affects young horses and static compression of the mid to caudal portion of the cervical spine (from C5 through C7) associated with articular process (AP) joint arthropathy that affects horses of various ages.

Radiography of the cervical spine and radiographic myelography of the cervical spinal cord are commonly used to identify the cause of ataxia.[4] However, the dimension of the vertebral canal can best be evaluated in only a sagittal plane with these diagnostic imaging modalities, and they are associated with false positive and false negative results.[3–6] Alternatively, CT myelography (CTM) and MRI are the best diagnostic imaging modalities to evaluate for and identify the cause of spinal cord compression in companion animals.[9,10] For horses examined with MRI postmortem, the ratio of vertebral canal area to spinal cord canal area was more accurate to detect vertebral canal stenosis and spinal cord compression that was confirmed with histologic examination, compared with intra- and intervertebral ratios for minimal sagittal diameter.[6] In another study,[11] CTM was performed for 5 Thoroughbred foals, and the quotient of the area of the cervical spinal cord divided by the area of the subarachnoid space plus the cervical spinal cord was used to quantify the degree of spinal cord compression and compare with histologic examination findings. More recently, the features of cervical spinal CT and CTM have been described in 3 large retrospective studies.[12–14] Yet none of these studies focused on the evaluation of ataxic horses with CTM, objective quantification of the degree of spinal cord compression, or associations between the location and direction of compression or between the size of an AP and degree of compression.

Therefore, the objectives of the retrospective study reported here were to characterize CTM find-

Unauthenticated | Downloaded 07/16/24 03:48 PM UTC

ings of the cervical spine in ataxic horses, quantify the degree of dural compression (ratio of the cross-sectional area of the cervical spinal cord and the total cross-sectional area of the subarachnoid space plus the cervical spinal cord), and determine whether associations existed between the location and direction of the compression or between the size of the APs and the degree of compression. The hypotheses were that associations existed between the location and direction of the compression and between the size of the APs and the degree of compression.

Materials and Methods

Animals

All horses with ataxia of all limbs that underwent CTM of the cervical spine between January 2015 and January 2017 were eligible for inclusion in this retrospective study. Age, body weight, breed, sex, degree of ataxia, and CTM findings were retrieved from the medical records. Physical examination was performed by one of the authors (EA or TM). A scale of 0 to 5 was used to grade the severity of ataxia.[15]

CTM image acquisition

Non–contrast-enhanced CT images were acquired before CTM images were acquired. Horses were anesthetized and positioned in right lateral recumbency, with the neck in a horizontal, neutral position, for image acquisition with a standard-bore (diameter, 72 cm), 4-slice, third-generation CT machine. The CT machine had a limited amount of hardware between a horse's shoulders and the bore, which made acquisition of images of the caudal region of the cervical spine possible. The scanning parameters were as follows: 135 kVp, 200 mA, collimator pitch of 1.1, detector pitch of 4.5, 1-mm slice thickness, 1-mm reconstruction interval, matrix size of 512 X 512 pixels, and field of view of 400 mm. The bone or soft tissue filter was applied, and images were acquired from the occiput through T1. Two scans were necessary to image the entire cervical spine: one from the occiput through C3 and another from C3 through T1.

For CTM image acquisition, the subarachnoid space was punctured at the atlanto-occipital joint, 50 mL of CSF was removed, and 30 mg of iodine/kg of iohexol (300 mg of iodine/mL) was injected with an aseptic technique and ultrasound guidance.[16] To increase the caudal movement of iohexol, the horse's head was elevated for 5 minutes after injection but prior to image acquisition. Removed CSF was not analyzed.

CTM image interpretation

A board-certified equine radiologist (TR) who was blinded to patient history, physical examination findings, and prior CTM reports retrospectively reviewed CTM images on a dedicated workstation with a DICOM viewer (Osirix; Pixmeo SAR). Images were evaluated in bone (level, 500 HU; width, 1,500 HU) and soft tissue (level, 250 HU; width, 650 HU) windows. Two-dimensional transverse, sagittal, and dorsal planar images were made by use of multiplanar reconstruction. Evaluation of dural compression and all measurements were made from the transverse plane of the multiplanar reconstruction (plane perpendicular to the spinal cord, whereas the sagittal plane of the multiplanar reconstruction was the plane parallel to the vertebral spinous process). For the purpose of this study, a noncompressive site was defined as a site that did not have narrowing or had only mild flattening of the subarachnoid space.

All sites with > 50% compression of the subarachnoid space (when compared with noncompressive sites in the local region cranial or caudal to the site of dural compression) were recorded independent of the direction of the compression. At those sites, the location, direction (ie, dorsal, dorsolateral, lateral, ventrolateral, or ventral), cause (ie, the anatomical structure that caused narrowing of the contrast column), and type (ie, extradural, intradural extramedullary, or intradural intramedullary) of narrowing of the subarachnoid space were noted. Deviation of the spinal cord and presence of a modification in the shape of the spinal cord were assessed subjectively (when compared with noncompressive sites in the local region cranial or caudal to the site of dural compression). If > 1 direction of subarachnoid space compression was present at each site, the direction that caused the most compression was recorded.

To assess the degree of dural compression, a spinal cord-to-dura ratio was calculated; the ratio was defined as the ratio of the cross-sectional area of the spinal cord and the total cross-sectional area of the spinal cord plus the subarachnoid space. Cross-sectional areas were traced by hand by use of the closed polygon function of a DICOM viewer (Osirix; Pixmeo SAR). In all horses, the spinal cord-to-dura ratio was calculated at all sites (between 2 successive dorsal arches) from C2 through T1 that did exhibit compression and at all sites that had > 50% compression of the subarachnoid space. The spinal cord-to-dura ratio for noncompressive sites was calculated only at intervertebral locations because a preliminary study revealed that all sites of dural compression were at the intervertebral disk spaces or adjacent to the APs (data not shown) and because 2 previous studies[12,13] of horses that underwent CTM of the cervical spinal cord revealed that subarachnoid space compression was identified primarily at the intervertebral disk spaces or adjacent to the APs. For each horse, the site with the maximum spinal cord-to-dura ratio was considered to be the site of maximum dural compression.

A ratio, denoted as AP-to-vertebral body ratio (APBR), was derived to assess the size of the AP; the ratio was the cross-sectional area of the AP and the cross-sectional area of the largest part of the cranial aspect of the body of C6.[14] The ratio was calculated for all horses at all sites from C2 through T1 that had > 50% compression of the subarachnoid space.

Unauthenticated | Downloaded 07/16/24 03:48 PM UTC

Data analysis

At all sites that had > 50% compression of the subarachnoid space, linear regression analyses were performed to assess the effect of the size of the AP (determined with use of the APBR) on the degree of subarachnoid space compression. A linear regression model with spinal cord-to-dura ratio as the dependent variable and APBR (mean or maximum value between both sides at 1 location) as the independent variable was fitted, with slope as the summary statistic and the *P* value indicating whether the slope differs from zero. Additionally for the same sites with > 50% compression, the Fisher exact test was used to assess the effect of the site on the direction of the compression of the subarachnoid space (dorsal, dorsolateral, lateral, ventrolateral, or ventral). For this assessment, the cervical spine was divided into 3 parts: occiput through mid-C4, mid-C4 through mid-C6, and mid-C6 through mid-T1. All statistical analyses were performed with commercially available software (R version 3.6.3; R Foundation). Values of $P < 0.05$ were considered significant.

Results

Animals

Twenty-six horses met eligibility requirements and were included in the study. All horses were warmblood horses and located in Europe; no horse had a history of travel outside Europe. Eighteen (69%) horses were male (gelding, n = 10; stallion, 8), and 8 (31%) were female. Ages ranged from 0.25 to 17 years (mean, 6.3 years; median, 6 years), and body weight ranged from 173 to 632 kg (mean, 494.7 kg; median, 527 kg). Duration of clinical signs was variable (1 week to several years). Three horses had an episode of signs of severe neck pain, manifested by an inability to move their necks and the presence of neck ventroflexion. At presentation, all horses had signs of ataxia for all limbs; median grade of ataxia was 3 (range, 1 to 4). Images were acquired through CTM for all horses from the occiput through T1, and all horses had at least 1 site with > 50% compression of the subarachnoid space.

CTM findings

Spinal cord-to-dura ratio—A ratio could be calculated for all horses at all available noncompressive sites and sites with > 50% compression **(Table 1)**. Mean ± SD spinal cord-to-dura ratio was 0.31 ± 0.044 (range, 0.20 to 0.41) for noncompressive sites, 0.40 ± 0.076 (0.28 to 0.60) for sites with > 50% compression of the subarachnoid space, and 0.44 ± 0.078 (0.29 to 0.60) for sites with maximum dural compression.

Sites with > 50% compression of the subarachnoid space—Greater than 50% compression of the subarachnoid space was noted for 51 sites (1 to 3 sites/horse). All

Table 1—Spinal cord-to-dura ratios from C2 through T1 determined with CT myelography (CTM) between January 2015 and January 2017 for 26 client-owned warmblood horses with ataxia that affected all limbs. Note that the spinal cord-to-dura ratios for the site of maximum compression† for horses 4, 7, 11, and 13 was comparable to the ratios for the noncompressive sites. Findings of CTM for these 4 horses were considered unremarkable.

Horse	C2 through C3	C3 through C4	C4 through C5	C5 through C6	C6 through C7	C7 through T1
1	0.26	0.33*	0.29	0.31	0.34	0.40†
2	0.33	0.33*	0.32	0.53†	0.33	0.32
3	0.27	0.30*	0.31	0.33	0.45†	0.30
4	0.27	0.30†	0.28	0.31	0.26	0.22
5	0.35	0.40*	0.36	0.44†	0.36	0.32
6	0.30	0.33	0.34	0.36	0.44†	0.29
7	0.22	0.30†	0.31	0.32	0.33	0.32
8	0.33	0.41*	0.34	0.45*	0.48†	0.26
9	0.33	0.55†	0.32	0.32	0.29	0.31
10	0.26	0.33*	0.35*	0.34	0.43†	0.29
11	0.30†	0.30	0.33	0.28	0.31	0.26
12	0.30	0.30	0.29	0.35	0.42†	0.23
13	0.29†	0.23	0.27	0.28	0.28	0.23
14	0.26	0.31	0.29	0.36*	0.33	0.42†
15	0.33	0.54†	0.35	0.33	0.33	0.44*
16	0.27	0.38*	0.29	0.28	0.46†	0.32
17	0.36	0.44*	0.46†	0.36	0.36	0.31
18	0.35	0.38	0.38	0.34	0.43*	0.49†
19	0.29	0.34	0.35	0.48†	0.43*	0.30
20	0.46†	0.36	0.37	0.35	0.35	0.32
21	0.35	0.30	0.27	0.29	0.48†	0.28
22	0.27	0.37*	0.31	0.33	0.40†	0.29
23	0.28	0.29	0.29	0.31	0.49†	0.23
24	0.27	0.43†	0.37*	0.34*	0.33	0.28
25	0.26	0.28	0.27	0.28	0.44†	0.25
26	0.32	0.60†	0.35	0.37	0.38	0.37

*Indicates site had > 50% compression of the subarachnoid space but was not the site of maximum compression. †Indicates site of maximum compression of the subarachnoid space.

Unauthenticated | Downloaded 07/16/24 03:48 PM UTC

51 sites were at intervertebral disk spaces or adjacent to the APs, and compression was extradural **(Table 2)**. The most common site was C3 through C4 (n = 16). The other sites were C6 through C7 (13), C5 through C6 (6), C2 through C3 (5), C7 through T1 (4), the atlanto-occipital joint (4), and C4 through C5 (3). Ventral was the most common direction of maximum compression (n = 22), followed by lateral (12), dorsolateral (10), and dorsal (7). Ventrolateral direction was not identified. Ventral compression of the subarachnoid space was caused by dorsal extension of the adjacent intervertebral disk **(Figure 1)**. Lateral compression of the subarachnoid space was caused by an enlarged AP (8/12 sites) or contact with the most dependent (right) occipital condyle

Table 2—Age and sex (F, mare; M, stallion; MC, gelding) and, identified with CTM, site, direction of the compression, compressing structure, spinal cord-to-dura ratio, and spinal cord shape (A, abnormal; N, normal) at the sites of maximum dural compression, defined as the site with the largest spinal cord-to-dura ratio, for each horse of Table 1.

Horse	Age (y)	Sex	Site	Direction of compression	Compressing structure	Spinal cord-to-dura ratio	Spinal cord shape
1	2	M	C7 through T1	Dorsolateral (unilateral)	Enlarged left AP	0.40	N
2	9	MC	C5 through C6	Dorsolateral (unilateral)	New bone formation of the cranial dorsal arch and asymmetric soft tissue proliferation at this level with fissure and sclerosis of the spinous process of C6	0.53	A
3	9	MC	C6 through C7	Dorsolateral (bilateral)	Enlarged left and right APs	0.45	A
4	6	MC	C3 through C4	Ventral	Intervertebral disk protrusion with gas attenuation within the disk	0.30	N
5	2	MC	C5 through C6	Ventral	Intervertebral disk protrusion	0.44	A
6	17	F	C6 through C7	Dorsolateral (unilateral)	Soft tissue attenuation medial to the left AP	0.44	N
7	10	F	C3 through C4	Ventral	Intervertebral disk protrusion	0.30	N
8	4	MC	C6 through C7	Lateral (unilateral)	Enlarged left AP	0.48	N
9	7	F	C3 through C4	Dorsolateral (unilateral)	Enlarged right AP	0.55	N
10	6	MC	C6 through C7	Dorsal	New bone formation of the cranial aspect of the dorsal arch of C7	0.43	N
11	6	MC	C2 through C3	Ventral	Intervertebral disk protrusion	0.30	N
12	4	M	C6 through C7	Dorsolateral (unilateral)	Soft tissue attenuation medial to the right AP	0.42	A
13	8	M	C2 through C3	Ventral	Intervertebral disk protrusion	0.29	N
14	1	M	C7 through T1	Dorsolateral (unilateral)	Enlarged right AP	0.42	N
15	1	F	C3 through C4	Lateral (bilateral)	Enlarged left and right APs	0.54	A
16	6	MC	C6 through C7	Ventral	Intervertebral disk protrusion	0.46	N
17	17	F	C4 through C5	Ventral	Intervertebral disk protrusion with gas attenuation within the disk	0.46	A
18	2	M	C7 through T1	Dorsal	Cranial aspect of the dorsal arch of T1	0.49	N
19	1	M	C5 through C6	Dorsolateral	Soft tissue attenuation medial to the left AP	0.48	A
20	9	F	C2 through C3	Ventral	Intervertebral disk protrusion	0.46	N
21	5	F	C6 through C7	Dorsolateral (unilateral)	Soft tissue attenuation medial to the left AP	0.48	A
22	8	F	C6 through C7	Dorsolateral (unilateral)	Soft tissue attenuation medial to the left AP	0.40	A
23	8	MC	C6 through C7	Ventral	Intervertebral disk with collapse of the intervertebral disk space	0.49	A
24	7	MC	C3 through C4	Ventral	Intervertebral disk protrusion	0.43	A
25	2	M	C6 through C7	Ventral	Intervertebral disk protrusion	0.44	N
26	0.25	M	C3 through C4	Lateral (bilateral)	Enlarged left and right APs	0.60	A

AP = Articular process.

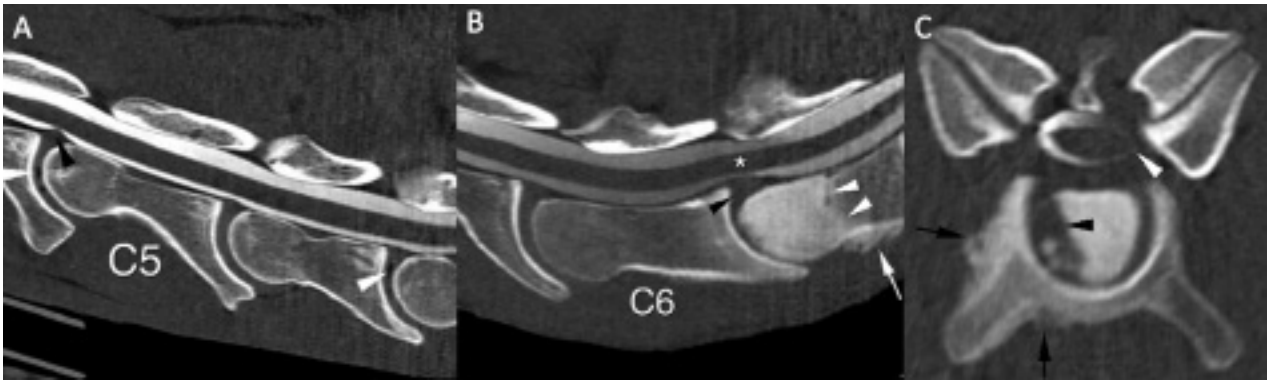

Figure 1—Images acquired with CT myelography (CTM; in bone window) of sites of ventral dural compression for 2 horses. A—Midsagittal reconstructed image of C4 through C6 for horse 17. Cranial is to the left of the image. In comparison with the other intervertebral disks, note dorsal protrusion of the C4-5 disk and subsequent ventral dural compression (black arrowhead). Also note gas attenuation in the C4-5 and C6-7 disks (white arrowheads). B—Midsagittal reconstructed image of C5 through C7 for horse 23. Cranial is to the left of the image. Note severe decreased thickness of the intervertebral symphysis of C6 through C7, dorsal protrusion of the C6-7 disk (black arrowhead), and subsequent ventral dural compression and dorsal deviation of the spinal cord (asterisk) as well as severe increased attenuation of the cranial one-half of the body of C7 (white arrowheads) with new bone formation ventrally (arrow). C—Transverse image of C6 through C7 of the same horse in panel B. Ventral dural compression is more severe on the left side (white arrowhead), a feature that is not conspicuous in panel B and may be missed with radiographic myelography. Also note dorsoventral flattening of the spinal cord, lysis of the right and cranial aspects of the body of C7 (black arrowhead), and new bone formation of the right and caudal aspects of the body of C6 (black arrows). These abnormalities are compatible with previous trauma or infection.

Unauthenticated | Downloaded 07/16/24 03:48 PM UTC

at the atlanto-occipital joint (4/12 sites; **Figure 2**). Dorsolateral compression of the subarachnoid space was caused by an adjacent enlarged AP (5/10 sites) or soft tissue–attenuating material medial to the AP (5/10 sites; **Figures 3 and 4**). Dorsal compression of the subarachnoid space was caused by direct impingement by the cranial aspect of the dorsal arch (5/7 sites) or impingement by soft tissue–attenuating material cranial or ventral to the cranial aspect of the dorsal arch (2/7 sites).

Sites of maximum dural compression—The most common site of maximum compression was C6 through C7 (n = 10), followed by C3 through C4 (6), C5 through C6 (3), C7 through T1 (3), C2 through C3 (3), and C4 through C5 (1). Hence, 16 of the 26 (61.5%) sites of maximum compression were identified in the caudal portion of the cervical spine (C5 through T1). Dorsolateral or lateral compression was identified in 13 (50%) sites, followed by ventral (11) and dorsal (2). Dorsolateral or lateral compression was caused by enlargement of the APs at 7 sites, soft tissue–attenuating material medial to the APs at 5 sites, or a combination of new bone formation and soft tissue proliferation at the cranial aspect of the dorsal arch at 1 site (Figures 1–3). Ventral compression was caused by dorsal protrusion of the adjacent intervertebral disk (Figure 4).

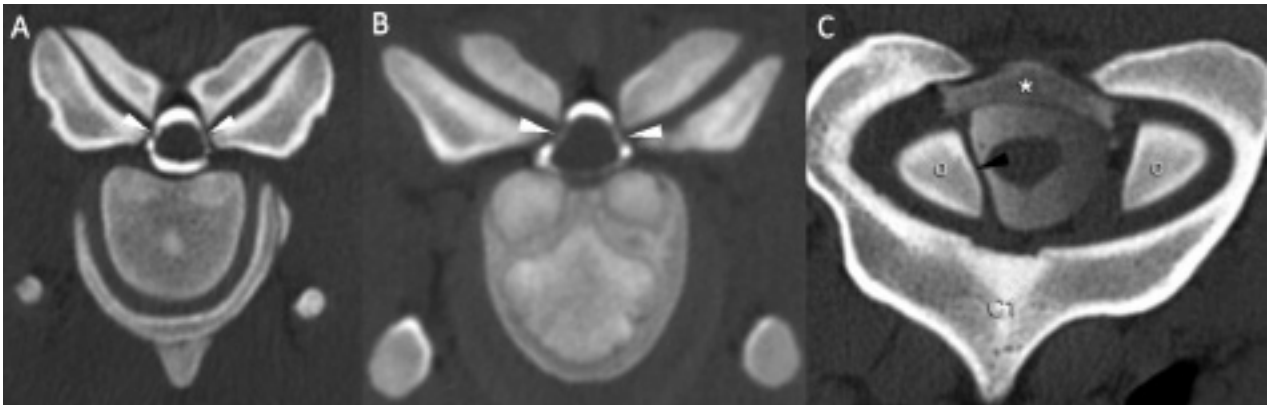

Figure 2—Images acquired with CTM (in bone window) of sites of lateral dural compression for 3 horses. Right is to the left of the image. A—Transverse image of C3 through C4, the site of maximum dural compression, for horse 15. Note bilateral compression caused by both articular processes (APs; arrowheads) and abnormal round shape and increased height of the spinal cord. B—Transverse image of C3 through C4, the site of maximum dural compression, for horse 26. Note bilateral compression caused by both APs (arrowheads) and the abnormal triangle shape of the spinal cord. C—Transverse image of the atlanto-occipital joint for horse 3. Note lateral compression of the dura by the right occipital condyle (O; arrowhead), which was considered to be an incidental finding because it was seen on only the right (gravity-dependent) side (each horse was positioned in right lateral recumbency for CTM). Also note leakage of contrast material in the epidural space dorsally (asterisk). C1 = Atlas.

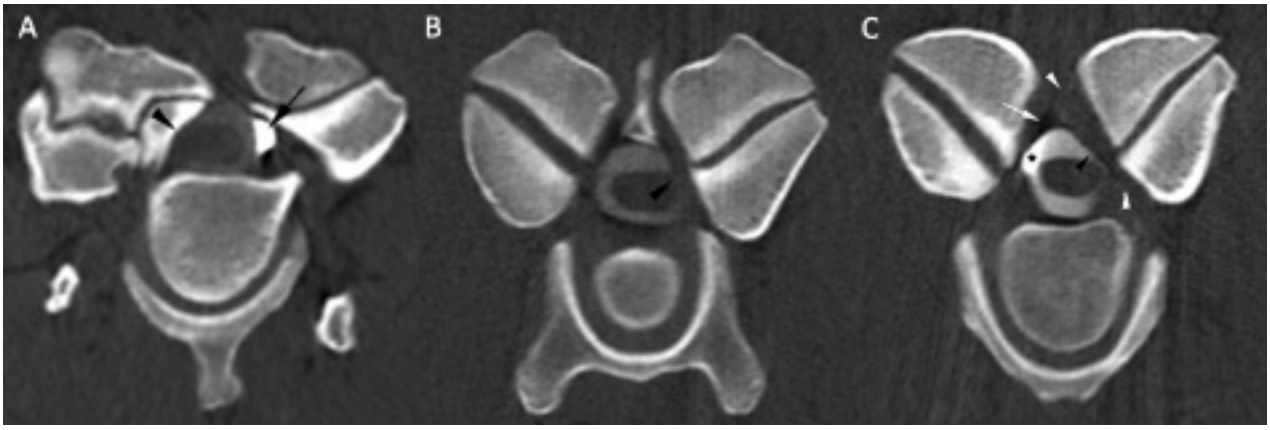

Figure 3—Images acquired with CTM (in bone window) of sites of dorsolateral dural compression. Right is to the left of the image. A—Transverse image of C3 through C4, the site of maximum compression, for horse 9. The right APs are large and misshapen, leading to dorsolateral compression (arrowhead), and are fragmented and have irregularities of the subchondral bone (not clearly visible on this image). Also note the leakage of contrast material in the epidural space (arrow). B—Transverse image of C6 through C7, the site of maximum compression, for horse 6. The left and right APs are large and round. On the left, dorsolateral compression (arrowhead) is noted owing to soft tissue–attenuating material between the left AP and the dural tube. C—Transverse image of C6 through C7, the site of maximum compression, for horse 22. The APs are large, and proliferated soft tissue (white arrowheads) is causing dorsolateral dural compression (black arrowhead). The epidural fat is conspicuous on the dorsal right side (arrow) but not the left side, most likely because of a mass effect from the soft tissue proliferation. Also note pooling of the contrast material on the right (asterisk), most likely because the right side was the gravity-dependent side (each horse was positioned in right lateral recumbency for CTM).

Unauthenticated | Downloaded 07/16/24 03:48 PM UTC

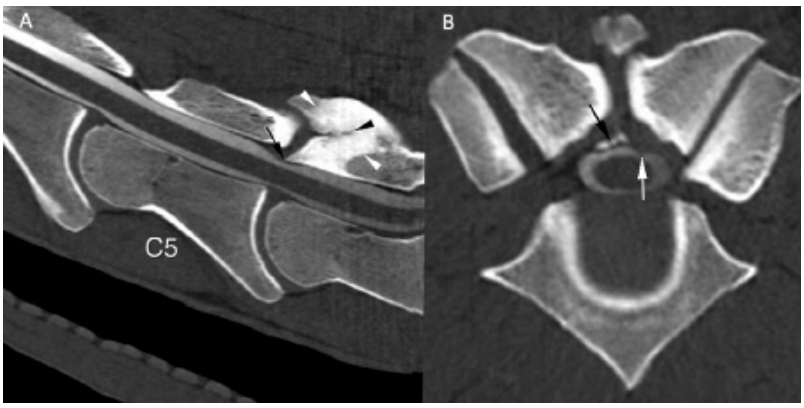

Figure 4—Images acquired with CTM (in bone window) of the site of maximum dural compression for horse 2. A—Midsagittal reconstructed image of C4 through C6. Cranial is to the left of the image. Note new bone formation of the cranioventral aspect of the dorsal arch of C6 (arrow) that created dorsal extradural compression of the subarachnoid space. Also note the ill-defined fragmentation of the spinous process of C6 (black arrowhead) surrounded by severe increased attenuation of the bone (white arrowheads), which is likely consistent with sclerosis. B—Transverse image of C5 through C6. Right is to the left of the image. Note the cranial tip of new bone formation (black arrow) of the cranial dorsal arch of C6 and soft tissue proliferation to the left of this new bone formation (white arrow) that created more severe dorsal compression (vs that seen in panel A) at this level. Changes seen in panel B are not seen in panel A and may be missed with a radiographic myelography, which assesses compression mostly in the midsagittal plane.

Table 3—Direction of compression of the sites that had > 50% compression of the subarachnoid space as identified with CTM for the horses of Table 1.

Site	Dorsal	Dorsolateral	Lateral	Ventral	Total
Occiput through C4	0	1	9	15	**25**
C4 through C6	2	1	2	4	**9**
C6 through T1	5	8	1	3	**17**
Total	**7**	**10**	**12**	**22**	

Dorsal compression was caused by direct impingement by the cranial aspect of the dorsal arch.

Abnormal shape and deviation of the spinal cord—In 13 of the 51 sites that had > 50% compression of the subarachnoid space, the shape of the spinal cord was considered abnormal in the transverse plane (Figures 3 and 4), with 12 identified at the site of maximum dural compression. Compression was dorsolateral at 6 of the 13 sites, ventral at 5, and lateral at 2. Eight of the 13 sites had a dorsal deviation of the spinal cord and ventral compression, with 7 of 8 identified at the site of maximum dural compression.

Subjective assessment of the clinical relevance—In 4 cases, > 50% of compression of the subarachnoid space was right lateralized, against the right occipital condyle (Figure 3), and these sites were never those of maximum compression. Consequently, this finding was considered clinically unimportant and instead was secondary to patient positioning in right lateral recumbency during the CTM examination. The dural tube was wide at this level owing to the proximity of the cisterna magna (cerebellomedullaris cistern),[17] and compression was always identified on the gravity-dependent (right) side.

In 4 horses (horses 4, 7, 11, and 13; Tables 1 and 2), the degree of maximum compression was considered mild, with spinal cord-to-dura ratios (range, 0.29 to 0.30) that were comparable to the ratios for noncompressive sites, and dorsal deviation or abnormal shape of the spinal cord was not evident. Therefore, clinically relevant static compression was considered unlikely, and the CTM findings were considered unremarkable. The site of maximum compression was identified at C2 through C4.

Effect of the location on the direction of dural compression—The direction of dural compression of all sites with > 50% of compression of the subarachnoid space was detailed **(Table 3)**. The directions from the occiput through C4 were primarily ventral and lateral, whereas directions from C6 through T1 were primarily dorsal and dorsolateral. These differences were significant ($P < 0.001$).

Effect of the size of the APs on the degree of dural compression—Mean ± SD APBR was 1.1 ± 0.31 (range, 0.48 to 2.4) for all sites that had compression of the subarachnoid space and 1.0 ± 0.24 (0.48 to 2.4) for all sites that did not have compression of the subarachnoid space. The 4 sites of compression identified at the occipital condyle were excluded from the analysis because calculation of the APBR at this location was not possible. Determined with linear regression analyses, mean ($P = 0.5$) or maximum ($P = 0.6$) APBR did not have a significant effect on the degree of dural compression.

Discussion

The retrospective study reported here revealed that CTM of the cervical spine of ataxic horses was able to help identify the structure that caused dural compression and the direction of maximum compression, quantify the degree of compression, and determine whether associations existed between the location and direction of the compression or between the size of the APs and the degree of compression. The hypotheses were that associations existed between the location and direction of the compression and between the size of the APs and the degree of compression, but an association was detected only for the former.

Males were overrepresented, possibly explained by a predisposition of males to develop CCM as previously reported[18,19] or by the relatively small number of horses in the present study, such that this finding may not be representative of the general population. Yet males were also overrepresented in other CT and CTM studies[12–14] of the cervical spinal area for horses.

Unauthenticated | Downloaded 07/16/24 03:48 PM UTC

In the present study, CTM was able to help identify dorsolateral and lateral extradural compression as the directions of maximum compression. The anatomical pathways involved in CCM are the general proprioceptive tracts (spinocerebellar tracts).[7] Because these tracts are superficial, lateral, and dorsolateral in the white matter of the spinal cord,[7,17] detection of lateral and dorsolateral compressive lesions is essential. Lateral and dorsolateral compression may be overlooked with radiographic myelography, which mostly detects dorsoventral compression because laterolateral views are usually obtained, whereas oblique views are difficult to obtain and assess.

The site of maximum compression had dorsolateral (n = 10) or lateral (3) compression in 50% of the horses in the present study. At these sites, causes of compression were enlarged APs (dorsolateral compression, 4; lateral compression, 3), soft tissue–attenuating material medial to an enlarged AP (dorsolateral compression, 5), or new bone formation at the cranial aspect of the dorsal arch and asymmetric soft tissue proliferation at this level (dorsolateral compression, 1). In a previous study,[12] 63% of all sites of contrast attenuation identified with CTM were caused by pathologic changes to the APJs. In the present study, 46% of the maximum sites (12/26) were caused by pathologic changes of the APJs. Enlargement of the APs of the cervical spine for horses is a feature of degenerative joint disease[1,20] or vertebral malformation.[21,22] The soft tissue–attenuating material identified between the AP and dura may represent a synovial cyst, fibrovascular or fibrocartilaginous proliferation of the AP joint capsule, or a ligamentum flavum.[7,23] In the present study, the most common site of maximum compression was C6 through C7. This finding is similar to the result of 2 studies,[12,13] in which C6 through 7 was identified as the most common site of compression. Not all sites of > 50% compression of the subarachnoid space are believed to be associated with clinically relevant compression, especially at ventral sites of narrowing. Nevertheless, the spinal cord-to-dura ratios for all sites that had > 50% compression of the subarachnoid space were calculated. This decision was based on the fact that some horses may have maximum compression primarily from a ventral direction with additional directions of compression and on the results of a CTM study[11] of ataxic Thoroughbred foals that indicate ventral compression as the primary direction of compression. Moreover, > 50% compression of the subarachnoid space was used to define a moderate grade of compression in CTM in a previous study,[13] and interestingly, 12% of all sites of spinal cord impingement identified in a cervical CTM study[12] of 125 horses were dorsal to intervertebral disks.

In 4 cases (horses 4, 7, 11, and 13), clinically relevant static compression at the site of maximum compression was considered unlikely and CTM findings were considered to be unremarkable. In those cases, the site of maximum compression was ventral for C2 through C4. A possible explanation for this result was that dynamic compression could not be assessed because the neck could not be flexed or extended during CTM. Inability to acquire images with dynamic compression was a limitation of the present study and is likely a limitation of the usefulness of CTM in horses. Therefore, radiographic myelography with flexion and extension of the neck may be informative when the results of CTM are negative or equivocal. Radiographic myelography is also advised by authors of a recent study[13] to avoid underestimating the degree of compression identified with CTM. However, flexion of the neck during radiographic myelography increases the frequency of a false positive diagnosis of a lesion affecting the midcervical spinal region.[5]

Other causes of lesions of the cervical spinal cord, such as a trauma, degenerative myeloencephalopathy, equine protozoal myeloencephalopathy, equine herpesvirus 1 myeloencephalopathy and other viral myeloencephalopathies,[7] and a lesion cranial to the foramen magnum, could not be excluded for all cases and could have explained the clinical signs of the aforementioned 4 cases. Serum biochemical analyses, including pre- and postprandial bile acids analyses, were not performed to screen for hepatic encephalopathy, and CSF analysis was not performed.[7] However, no horse had a confirmed episode of hyperthermia, and equine protozoal myeloencephalopathy was considered unlikely because it is of low prevalence in Europe, all horses resided in Europe without a history of travel, and equine protozoal myeloencephalopathy seems restricted to horses that return or are imported from North America.[24]

The spinal cord-to-dura ratio was selected to objectively quantify the degree of compression in the present study. At noncompressive sites, the ratio was between 0.22 and 0.38, whereas at sites of maximum compression, the ratio was between 0.29 and 0.60. With exclusion of the 4 horses that had unremarkable CTM examinations, the ratio was between 0.40 and 0.60. These ratios were less than that previously reported[11] for 6 Thoroughbred yearlings. Possible explanations for this discrepancy are differences in the methods to determine these ratios or the fact that younger horses normally have higher ratios; the mean age of the horses in the present study was 6.3 years. A ratio > 0.52 to 0.54 is reported[11] to be suggestive for compression of the spinal cord. In the present study, a cutoff value for the ratio that distinguished between compressive and noncompressive sites could not be determined because of the lack of postmortem examinations.

At the site of maximum ventral compression in horses 4 and 17, the intervertebral disk protruded and had several gas attenuations. In people, this finding, sometimes referred to as vacuum phenomenon, is commonly reported secondary to degenerative changes but may also be incidental.[25] Other possible causes include infection, trauma, and neoplasia.[25,26] Gas accumulation was likely attributable to degenerative changes of the intervertebral disks.

At the site of maximum dorsolateral compression in horse 2, cranioventral new bone formation of the dorsal arch was associated with fissure of the spinous process of C6 that was surrounded by severe increased attenuation of bone and asymmetric soft tissue swelling. On the basis of a literature search, fissure of the dorsal arch of a cervical vertebra has not been previously reported in horses. Whether a relationship existed between fissure and new bone formation in this horse is unknown. Fragmentation of the spinous pro-

Unauthenticated | Downloaded 07/16/24 03:48 PM UTC

cess of C7 has been previously reported,[1] likely owing to trauma during neck extension. Trauma was also suspected as the cause of fissure in horse 2.

A critical limitation of the present study was the lack of a portmortem examination of the spinal cord to confirm the diagnosis of CCM or that, if a postmortem examination was performed, results could not be obtained. This was likely because the study was retrospective. However, the objective of the present study was to describe the CTM findings for ataxic horses, not to correlate the CTM findings with postmortem data. Also, transcranial electric or magnetic stimulation was not used in the horses in this study despite that these techniques may be useful to evaluate the functional integrity of spinal motor tracts and nerve conduction pathways. These techniques may also be useful in the future for helping to specify the location of the functional deficit that is causing ataxia[27] and to determine which compression site is clinically relevant when several compressive sites are identified with CTM.

In conclusion, the present study revealed the CTM findings of ataxic horses. Computed tomographic myelography was useful to identify the cause of dural compression, quantify the degree of compression, and identify the direction of compression. In a limited number of horses, the degree of static compression was considered unlikely to explain the clinical signs. Further studies are necessary to correlate CTM findings with histologic findings and to identify objective and reliable CTM decision criteria to differentiate horses with CCM from those without CCM.

Acknowledgments

No external funding was used in this study. The authors declare that there were no conflicts of interest.

The authors thank Drs. Taylor and Houdellier for their contributions to this study.

References

1. Dyson SJ. Lesions of the equine neck resulting in lameness or poor performance. *Vet Clin North Am Equine Pract*. 2011;27(3):417–437. doi:10.1016/j.cveq.2011.08.005
2. Estell K, Spriet M, Phillips KL, Aleman M, Finno CJ. Current dorsal myelographic column and dural diameter reduction rules do not apply at the cervicothoracic junction in horses. *Vet Radiol Ultrasound*. 2018;59(6):662–666. doi:10.1111/vru.12662
3. Hahn CN, Handel I, Green SL, Bronsvoort MB, Mayhew IG. Assessment of the utility of using intra- and intervertebral minimum sagittal diameter ratios in the diagnosis of cervical vertebral malformation in horses. *Vet Radiol Ultrasound*. 2008;49(1):1–6. doi:10.1111/j.1740-8261.2007.00308.x
4. Hahn CN. Cervical vertebral malformation. In: Reed SM, Bayly WM, Sellon DC, eds. *Equine internal medicine*. 3rd ed. Saunders Elsevier; 2010:603–606.
5. van Biervliet J, Scrivani PV, Divers TJ, Erb HN, de Lahunta A, Nixon A. Evaluation of decision criteria for detection of spinal cord compression based on cervical myelography in horses: 38 cases (1981–2001). *Equine Vet J*. 2004;36(1):14–20. doi:10.2746/0425164044864642
6. Janes JG, Garrett KS, McQuerry KJ, et al. Comparison of magnetic resonance imaging with standing cervical radiographs for evaluation of vertebral canal stenosis in equine cervical stenotic myelopathy. *Equine Vet J*. 2014;46(6):681–686. doi:10.1111/evj.12221
7. Nout YS, Reed SM. Cervical vertebral stenotic myelopathy. *Equine Vet Educ*. 2010;15(4):212–223. doi:10.1111/j.2042-3292.2003.tb00246.x
8. Powers BE, Stashak TS, Nixon AJ, Yovich JV, Norrdin RW. Pathology of the vertebral column of horses with cervical static stenosis. *Vet Pathol*. 1986;23(4):392–399. doi:10.1177/030098588602300408
9. da Costa RC, Echandi RL, Beauchamp D. Computed tomography myelographic findings in dogs with cervical spondylomyelopathy. *Vet Radiol Ultrasound*. 2012;53(1):64–70. doi:10.1111/j.1740-8261.2011.01869.x
10. Lipsitz D, Levitski RE, Chauvet AE, Berry WL. Magnetic resonance imaging features of cervical stenotic myelopathy in 21 dogs. *Vet Radiol Ultrasound*. 2001;42(1):20–27. doi:10.1111/j.1740-8261.2001.tb00899.x
11. Yamada K, Sato F, Hada T, et al. Quantitative evaluation of cervical cord compression by computed tomographic myelography in Thoroughbred foals. *J Equine Sci*. 2016;27(4):143–148. doi:10.1294/jes.27.143
12. Lindgren CM, Wright L, Kristoffersen M, Puchalski SM. Computed tomography and myelography of the equine cervical spine: 180 cases (2013–2018). *Equine Vet Educ*. 2021;33(9):475–483. doi:10.1111/eve.13350
13. Gough SL, Anderson JDC, Dixon JJ. Computed tomographic cervical myelography in horses: technique and findings in 51 clinical cases. *J Vet Intern Med*. 2020;34(5):2142–2151. doi:10.1111/jvim.15848
14. Rovel T, Zimmerman M, Duchateau L, et al. Computed tomographic examination of the articular process joints of the cervical spine in warmblood horses: 86 cases (2015–2017). *J Am Vet Med Assoc* 2021;259:1178–1187.
15. Mayhew IG, deLahunta A, Whitlock RH, Krook L, Tasker JB. Spinal cord disease in the horse. *Cornell Vet*. 1978;68(suppl 6):1–207.
16. Audigié F, Tapprest J, Didierlaurent D, Denoix JM. Ultrasound-guided atlanto-occipital puncture for myelography in the horse. *Vet Radiol Ultrasound*. 2004;45(4):340–344. doi:10.1111/j.1740-8261.2004.04065.x
17. Dyce KM, Sack WO, Wensing CJG. The nervous system. In: Dyce KM, Sack WO, Wensing CJG, eds. *Textbook of Veterinary Anatomy*. 4th ed. Saunders Elsevier; 2010:268–331.
18. Levine JM, Adam E, MacKay RJ, Walker MA, Frederick JD, Cohen ND. Confirmed and presumptive cervical vertebral compressive myelopathy in older horses: a retrospective study (1992–2004). *J Vet Intern Med*. 2007;21(4):812–819.
19. Levine JM, Ngheim PP, Levine GJ, Cohen ND. Associations of sex, breed, and age with cervical vertebral compressive myelopathy in horses: 811 cases (1974–2007). *J Am Vet Med Assoc*. 2008;233(9):1453–1458. doi:10.2460/javma.233.9.1453
20. Down SS, Henson FMD. Radiographic retrospective study of the caudal cervical articular process joints in the horse. *Equine Vet J*. 2009;41(6):518–524. doi:10.2746/042516409X391015
21. Moore BR, Reed SM, Robertson JT. Surgical treatment of cervical stenotic myelopathy in horses: 73 cases (1983–1992). *J Am Vet Med Assoc*. 1993;203(1):108–112.
22. Janes JG, Garrett KS, McQuerry KJ, et al. Cervical vertebral lesions in equine stenotic myelopathy. *Vet Pathol*. 2015;52(5):919–927. doi:10.1177/0300985815593127
23. van Biervliet J, Mayhew J, de Lahunta A. Cervical vertebral compressive myelopathy: diagnosis. *Clin Tech Equine Pract*. 2006;5(1):54–59. doi:10.1053/j.ctep.2006.01.010
24. Furr M. Equine protozoal myeloencephalitis. In: Reed SM, Bayly WM, Sellon DC, eds. *Equine Internal Medicine*. 3rd ed. Saunders Elsevier; 2010:609–616.
25. Samuel E. Vacuum intervertebral discs. *Br J Radiol*. 1948;21(247):337–339. doi:10.1259/0007-1285-21-247-337
26. Morishita K, Kasai Y, Uchida A. Clinical symptoms of patients with intervertebral vacuum phenomenon. *Neurologist*. 2008;14(1):37–39. doi:10.1097/NRL.0b013e3180dc9992
27. Journée SL, de Meeus d'Argenteuil C, De Maré L, et al. State-of-the-art diagnostic methods to diagnose equine spinal disorders, with special reference to transcranial magnetic stimulation and transcranial electrical stimulation. *J Equine Vet Sci*. 2019;81:102790. doi:10.1016/j.jevs.2019.102790

Unauthenticated | Downloaded 07/16/24 03:48 PM UTC